Order-Disorder Phase Transition and Critical Slowing Down in Photorefractive Self-Oscillators

Doruk Engin,[1] Sergei Orlov,[1] Mordechai Segev,[2] George C. Valley,[3] and Amnon Yariv[1]
[1]*California Institute of Technology, 128-95, Pasadena, California 91125*
[2]*Department of Electrical Engineering and Center for Photonics and Optoelectronic Materials (POEM) and the Princeton Material Institute (PMI), Princeton University, Princeton, New Jersey 08544*
[3]*Hughes Research Laboratories, 3011 Malibu Canyon Road, Malibu, California 90265*
(Received 15 August 1994)

We study self-oscillation in a photorefractive double phase-conjugate mirror and show that it undergoes an order-disorder phase transition at a critical gain-threshold point. We present theoretical and experimental results on two key properties of this phase transition: critical slowing down and the characteristic order parameter. We show that the correlation distance of the refractive index variation responsible for the double phase conjugation changes abruptly from very small values (disorder, below threshold) to a large unique value (order, above threshold) determined primarily by the boundary conditions. Finally, we point out similarities and important differences between this combined light and matter phase transition and the mean field and Ginzburg-Landau theories.

PACS numbers: 42.65.Hw, 64.60.Cn

Phase transitions have been studied extensively over the past decades. Two of their characteristic properties are critical slowing down at a critical point and large change in an order parameter as the system goes through that point [1]. These effects are observed in ferromagnets, in ferroelectric materials, and in many other systems that change their actual structure (ordering) at a specific critical point [2] (phase transition, Curie temperature, etc.). Lasers go through a critical point at the threshold and exhibit the features characteristic of phase transitions [3,4]. Critical slowing down is also observed in bistable optical resonators [5,6].

Theoretically, some nonlinear wave-mixing processes are also expected to exhibit critical slowing down. Nonlinear self-oscillation, which can be obtained at sufficiently large nonlinear gain (coupling strength times interaction length) levels, is a good candidate for such an observation. For example, consider degenerate four-wave mixing [7], where two counterpropagating optical ("pump") beams interact in a nonlinear crystal with a third ("probe") beam. A fourth ("signal") beam, which is a phase-conjugate replica of the probe, is generated in the medium through the nonlinear process. The probe beam is amplified and the phase-conjugate signal is generated simultaneously (both at the expense of the pumps). At a very high gain level, *both* signal and probe beams are emitted even in the *absence* of an input probe beam [7]. The behavior at this point is called self-oscillation.

In this Letter we analyze a specific example of nonlinear self-oscillation, the photorefractive double phase-conjugate mirror (DPCM), and show that it exhibits a phase transition at the critical point of self-oscillation. We observe that both the nonlinear medium and the phases of the participating waves go from disorder below the critical point to order above it. The order parameter is associated with phase-conjugate reflectivity, and the correlation distance is associated both with the period of the nonlinear perturbation in the refractive index and with the bandwidth (temporal and angular) of the scattered waves. We describe experimental observations of these phase-transition effects associated with nonlinear self-oscillation [8]. We study these effects in a photorefractive self-oscillator, since high gain levels can be obtained and controlled in a relatively accurate manner. Our analysis, however, is general and can be straightforwardly extended to include all photorefractive self-oscillators, and, with some modifications, all nonlinear (electromagnetic) self-oscillators.

The double phase-conjugate mirror [9] consists of a photorefractive crystal where two mutually incoherent input beams indirectly interact and emerge as phase conjugates of each other (i.e., the beams exchange amplitude and inverted phase profiles). As the DPCM develops, the input beams fan and at the same time scatter from each other's fanning gratings. This process proceeds most efficiently if the beams diffract everywhere from a set of shared gratings, which is possible only if the beams are phase conjugates of each other throughout the entire volume [10]. Therefore, a selection mechanism in which common gratings are enhanced and nonoverlapping gratings are suppressed governs the evolution. Eventually, if the gain (average coupling coefficient times interaction length) is large enough, the interaction stabilizes in a double phase-conjugation form. Recently, we presented a theoretical model for the evolution of the DPCM and showed how it evolves from two arbitrary input beams and randomly scattered noise [11,12]. We predicted the existence of a fidelity threshold for the double-conjugation process and established the self-oscillatory behavior of the DPCM. Later, we presented experimental observations demonstrating the existence of such a fidelity threshold that depends on the feature size in the conjugated images [13].

0031-9007/95/74(10)/1743(4)$06.00

For understanding the self-oscillatory behavior and the critical slowing down, it is useful to recall the time-dependent one-dimensional analysis of the DPCM [9,14], which treats it as a four (plane) wave-mixing problem, in the configuration described in the inset of Fig. 1. The coupled equations for the complex amplitudes $A_i(z,t)$ $(i = 1,2,3,4)$ of the interacting waves are

$$\frac{\partial A_1}{\partial z} = ik\Delta n A_4, \quad \frac{\partial A_2^*}{\partial z} = ik\Delta n A_3^*,$$
$$\frac{\partial A_3}{\partial z} = -ik\Delta n A_2, \quad \frac{\partial A_4^*}{\partial z} = -ik\Delta n A_1^*, \qquad (1)$$

where $k = 2\pi/\lambda$ is the wave number, λ is the wavelength in vacuum, and $\Delta n(z)$ is the perturbation in the refractive index. These coupled wave equations are supplemented by an equation for the index perturbation

$$\tau \frac{\partial \Delta n}{\partial t} + \Delta n = (\gamma/I_T)(A_1A_4^* + A_2^*A_3), \qquad (2)$$

where $I_T = \sum_{j=1}^4 |A_j|^2$ is the sum of the wave intensities, the response time τ is inversely proportional to I_T, and γ is the nonlinear coupling coefficient which is imaginary in PR materials without external or photovoltaic field, thus enabling power exchange between beams [11]. The boundary and the initial conditions for Eqs. (1) are $A_2(z,0) = A_2(L,t) = A_{2\mathrm{in}}$, $A_4(z,0) = A_4(0,t) = A_{4\mathrm{in}}$, and $\Delta n(z,0) = 0$ (where L is the length of the crystal). For simplicity, we consider here only the symmetric case of $|A_{2\mathrm{in}}|^2 = |A_{4\mathrm{in}}|^2$, which is also the case of lowest threshold [9,12,13]. Since this 1D model cannot account for interaction with non-phase-matched (spatial) noise (that initiates the evolution of the DPCM [11]), it is convenient to assume a small level of phase-matched seed ε, that is $A_1(0,t) = \sqrt{\varepsilon}\,A_4(0,t)$ and $A_3(L,t) = \sqrt{\varepsilon}\,A_2(L,t)$. These equations were solved [9,14] and give the steady-state results [9] for the symmetric phase conjugate reflectivity $R = |A_1(L,t\to\infty)/A_2(L,t\to\infty)|^2 = |A_3(0,t\to\infty)/A_4(0,t\to\infty)|^2 = a^2$, where a (real) is related to γL by

$$a = \tanh[-a\gamma L/2] = \tanh[a\gamma L/(\gamma L)_c], \qquad (3)$$

in the limit $\varepsilon \to 0$, and we identify the critical value $(\gamma L)_c = -2$. At and above the critical value of gain a has a finite value even in the absence of seeding noise ($\varepsilon \to 0$).

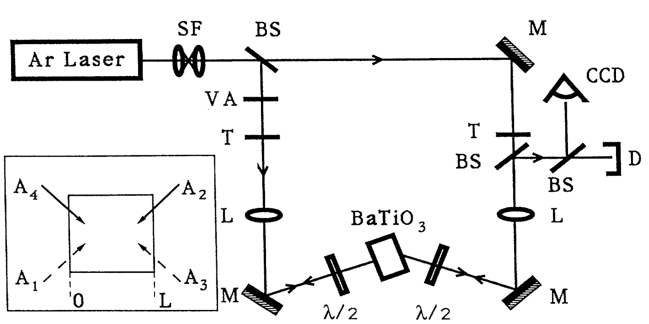

FIG. 1. The experimental setup. Inset: The DPCM configuration.

The transient solution [14] (for $a^2 \ll 1$) gives the characteristic time to reach steady state $T = \tau/[\gamma L - (\gamma L)_c]$. These two properties indicate self-oscillation ($R > 0$ for $\varepsilon \to 0$) and critical slowing down [$T \to \infty$ for $\gamma L \to (\gamma L)_c$].

The similarity to other systems that undergo second-order phase transitions is apparent from Eq. (3) which is analogous to the familiar expression in, for example, ferromagnetism [1,2]

$$M/M_\infty = \tanh[MT_C/M_\infty T] \qquad (4)$$

in the absence of external magnetic field, where M is the magnetization, M_∞ is the magnetization when all the spins are aligned, and T, T_C are the absolute and the Curie temperatures, respectively. This expression is obtained from the mean field theory, which treats the spin configuration as a bistate system in the absence of external magnetic field, and neglects all Fourier components of the spin except the mean (zero, in ferromagnetism). It minimizes the free energy function $F = -T\ln[2\cosh(MT_C/T)] + T_CM^2/2$. Its distinct property is that M is a continuous function of T everywhere (including at T_C), but its first derivative (which provides information about the entropy of the system) is discontinuous at T_C. In the case of DPCM, the free energy function is $F = -(1/\gamma L)\ln[2\cosh(a\gamma L/\gamma L_c)] + a^2/\gamma L_c$. The amplitude reflectivity a thus plays a role analogous to that of the magnetization M and is the "order parameter" of the system. The physical quantity which becomes "ordered" at the phase transition is the index $\Delta n(z)$ which assumes the form $\Delta n = \Delta n_0 \sin(2\pi z/\Lambda)$, $\Lambda = 2\pi/K_0 = \lambda/(2\sin\theta/2)$, where θ is the angle between the two input beams. This corresponds to a "condensation" in **K** space from a "broadband" to a near "monochromatic" behavior. For temperatures T above T_C in ferromagnetism, or for gain levels below $(\gamma L)_c$ for the DPCM, the system goes from order to disorder; that is, M and a vanish. To illustrate the equivalence between self-oscillation and second-order phase transition, we plot in Fig. 2(a) the two most distinct, common properties: the dependencies of the reflectivity R and the response time τ on the inverse of the gain $1/\gamma L$. The phase-transition behavior is manifested in the discontinuity of the first derivative of R with respect to $1/\gamma L$ and in the divergence of τ, both at $(\gamma L)_c$. An interesting point is the correspondence between the external magnetic field (H) in ferromagnetism and the noise seed level (ε), both taken to zero in the limit of $T \to T_C$ [or $\gamma L \to (\gamma L)_c$] in the mean field theory.

Our two-dimensional analysis [11,12] goes beyond mean field theory. It considers other possible Fourier components of the gratings, and in this sense is equivalent to the Ginzburg-Landau [1] theory of spin fluctuations. In the 1D model, the order parameter (a) represents the contribution of one single grating component K_0 (all others are neglected), and we examine its growth as a function of gain. In the 2D case one may look at the

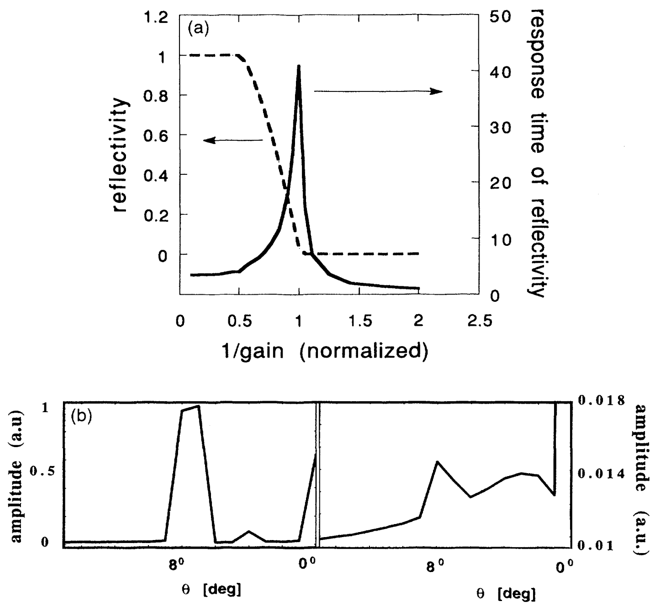

FIG. 2. (a) Numerical results of the 1D theory for the reflectivity (order parameter) and the time response, as a function of 1/gain. (b) Numerical results of the 2D theory: the spatial spectrum of one of the output beams *below* (right) and *above* (left) the threshold.

equivalent of "spin correlations." In the DPCM both the spectrum of the optical field and the spectrum of the refractive index perturbation show correlation effects. The field and the index are related: the narrower the spectral width of Δn, the smaller the allowed deviation from phase matching (Bragg condition). Figure 2(b) shows the spatial spectrum of one of the output beams below and above the critical point, as calculated from the 2D theory [11,12]. Below threshold multiple gratings coexist and the angular spectrum of the beam is broad (fanning), while above the threshold the preferential grating K_0 dominates, with only a small width associated with the features borne on the conjugated beam. This indicates a transition from disorder (broad spectral contents, low Bragg selectivity) to order (one dominant rating component, high selectivity).

We now present experimental results that illustrate the order-disorder phase transition. We use the setup shown in Fig. 1: a multimode 488-nm Ar-ion laser beam with a 3-cm coherence length passes through a spatial filter (SF) and is split by a beam splitter (BS) into two beams, which intersect in a photorefractive $BaTiO_3$ crystal. In each arm we place a transparency T (Air Force resolution chart), followed by another beam splitter (BS), a lens (L), and a half-wave plate. In one of the arms we insert a variable attenuator (VA). The phase conjugate reflections are collected by charge coupled device (CCD) cameras and detectors (D) from the beam splitters in each arm (the camera or detector system for the left arm is not shown in Fig. 1). Care is taken to assure that the beams are mutually incoherent at the crystal plane (the optical path difference between the arms is much larger than the coherence length). To facilitate an accurate control of the gain in the beams, it is essential to place the crystal between the image and the focal planes of the Air Force resolution chart so that the transverse intensity distribution in the crystal is nearly uniform [13]. The beams are nearly counterpropagating (172°) so that they fully overlap in the nonlinear crystal. In controlling the photorefractive gain, we recall [13] that additional illumination, incoherent with both interacting beams, reduces the modulation depth of the interference gratings and, consequently, decreases the resultant perturbation in the refractive index. Since in the current experiment we measure time response, it is essential to maintain the total illumination intensity at a constant value and as uniform as possible across the entire crystal. Since in $BaTiO_3$ the PR coupling is large for extraordinarily polarized light and negligible for ordinary polarization, we control the coupling by varying the polarization of the interacting beams. Thus, the ordinarily polarized portion of each beam serves as an erasure beam. Extraordinary polarization provides the highest gain, and ordinary polarization yields minimal gain. The coefficient γ may be expressed [13] as a function of the angle ϕ of the polarization of the input beams

$$\gamma(\phi) = \frac{\gamma_0}{1 + I_{\mathrm{ord}}/I_{\mathrm{ext}}} \approx \frac{\gamma_0}{1 + \tan^2\phi}, \tag{5}$$

where $\phi = 0$ corresponds to maximum gain (extraordinary polarization), and I_{ext} and I_{ord} are the sums of the intensities of the extraordinarily and ordinarily polarized beams, respectively. Note that the ordinarily polarized beams do not interact with each other or with the extraordinarily polarized beams, while the extraordinarily polarized beams form the DPCM and transform into each other's phase conjugates. This may result in a different spatial (x and z) dependence of I_{ord} and I_{ext}. Our choice for the interaction plane and the small angle between the beams minimizes this difference, and γ can be well approximated as a function of ϕ only, as in Eq. (5).

The experimental results are shown in Figs. 3 and 4. First we concentrate on a specific spatial frequency within the image. We block (using an aperture) the phase conjugate reflection of the entire image except for that of 3 bars (1.26 line pairs/mm). The phase-conjugate reflectivity R (normalized to its maximal value of 30%) and the response time in minutes as a function of gain are shown by the triangles and circles in Fig. 3. The response time reaches its maximal value exactly at the critical point of the reflectivity curve $[(\gamma L)_c \approx -2.06]$. The ratio between the response times at the threshold and at the highest gain is about 10. When the aperture is removed and the entire phase conjugate image is captured, we notice two effects. The first is the shift in the threshold value (which is also the gain value at the peak of the response time) toward higher gain levels for the whole phase-conjugate image. This is in accordance with our previous results [13] that show higher gain-threshold values for higher spatial frequencies. The second is the broadening of the

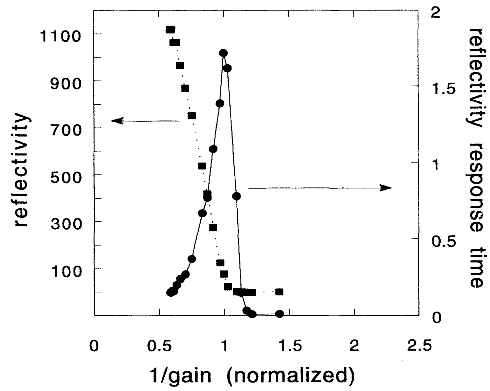

FIG. 3. Experimental results of the phase-conjugate reflectivity and time response as a function of gain for a single resolution image (1.26 line pairs/mm). The curves are a guide to the eye.

response time curve (for the whole image). This is a consequence of the different resolutions of the features incorporated in the Air Force resolution chart. Each spatial frequency in the image has a slightly different threshold, and consequently the response time averages and results in a slightly broader curve than in the single-resolution measurement.

To illustrate the change in the correlation distance when the DPCM goes through its threshold, we show in Fig. 4 experimental results (photographs, right column; profiles, left column) of the angular spectrum (far field) of one of the output beams below (upper sections) and above (lower sections) the transition point (threshold). It is evident that the spectrum narrows practically to a single Fourier component, broadened only by the pictorial information borne on the input beam. The behavior of the reflectivity, the response time, and the angular spectrum at the threshold are conclusive experimental evidence of a second-order phase transition.

Finally, we point out that the major difference between the nonlinear self-oscillator and other systems that undergo a phase transition is in the correlation distance. In all other phase transitions of which we are aware, the average Fourier component (or the mean value of the spin configuration [2], σ_0, or K_0 for the DPCM) is a given *property of the system.* In the self-oscillator case, it is given by the boundary conditions and is controlled by the angle between the input beams. Also our analysis can be readily extended to all photorefractive self-oscillators, which we believe all undergo a phase transition at their threshold. Furthermore, it is very likely that nonlinear self-oscillators that stem from other types of nonlinearities (for example, a Kerr self-oscillator [7]) also undergo a similar phase transition, since our treatment is rather general and does not require a specific form of the nonlinearity.

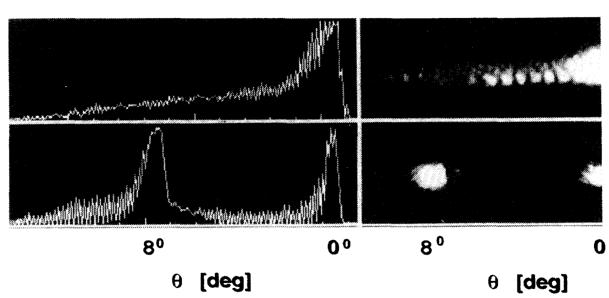

FIG. 4. Experimental results of the angular spectrum (far field) of one of the output beams below (upper section) and above (lower section) the transition point (threshold). The intensity of the small features in the upper right photograph is much smaller than the single (phase-conjugate) peak in the lower right photograph.

In conclusion, we have shown that photorefractive self-oscillation processes exhibit features of an order-disorder phase transition, and presented experimental observations of critical slowing down and correlation effects at the transition (threshold) point.

This study was supported by the Advanced Research Projects Agency, the Army Research Office, the Air Force Office of Scientific Research, and the Hughes Aircraft Company Internal Research and Development Program.

[1] L. D. Landau and E. M. Lifshitz, *Statistical Physics* (Pergamon Press, Oxford, 1958).

[2] R. Kubo, *Statistical Mechanics* (North-Holland, Amsterdam, 1965), Chap. 5, pp. 49–51.

[3] H. Haken, *Synergetics* (Springer-Verlag, New York, 1978), Chap. 8.

[4] K. Y. Lau, C. Harder, and A. Yariv, Appl. Phys. Lett. **40**, 198 (1982).

[5] R. Bonifacio and L. Lugiato, Opt. Commun. **19**, 172 (1976).

[6] E. Garmire, J. H. Marburger, S. D. Allen, and H. G. Winful, Appl. Phys. Lett. **34**, 374 (1979); H. A. Al-Attar, H. A. MacKenzie, and W. J. Firth, J. Opt. Soc. Am. B **3**, 1157 (1986).

[7] A. Yariv and D. M. Pepper, Opt. Lett. **1**, 16 (1977); see also A. Yariv, *Quantum Electronics,* 3rd ed. (John Wiley & Sons, New York, 1988), Chap. 17.

[8] A previous attempt to observe critical slowing down (without referring to any other critical phenomena) in a different type of photorefractive self-oscillator was made by D. A. Fish, T. J. Hall, and A. K. Powell, Opt. Commun. **84**, 85 (1991). An increase of the response time with increasing gain was reported, yet gain levels above the critical point could not be reached.

[9] S. Weiss, S. Sternklar, and B. Fischer, Opt. Lett. **12**, 114 (1987).

[10] M. Segev and A. Yariv, Opt. Lett. **16**, 1938 (1991).

[11] M. Segev, D. Engin, A. Yariv, and G. C. Valley, Opt. Lett. **18**, 1828 (1993).

[12] D. Engin, M. Segev, S. Orlov, A. Yariv, and G. C. Valley, J. Opt. Soc. Am. B **11**, 1708 (1994).

[13] S. Orlov, M. Segev, A. Yariv, and G. C. Valley, Opt. Lett. **19**, 578 (1994).

[14] V. V. Eliseev, V. T. Tikhonchuk, and A. A. Zozulya, J. Opt. Soc. Am. B **8**, 2497 (1991).

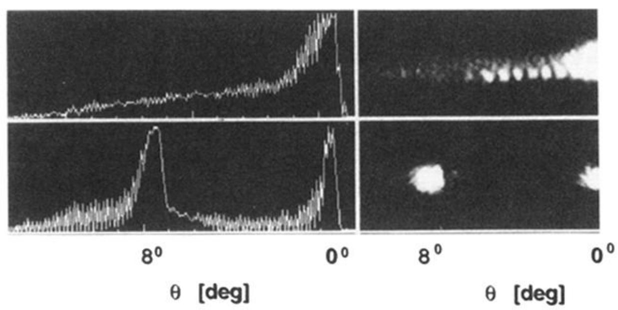

FIG. 4. Experimental results of the angular spectrum (far field) of one of the output beams below (upper section) and above (lower section) the transition point (threshold). The intensity of the small features in the upper right photograph is much smaller than the single (phase-conjugate) peak in the lower right photograph.